The resistive component $r_{\rm int}$ of the internal impedance in the classical model is negligible for a typical synchronous generator, but we found that it was non-negligible for our generators. We measured both the resistive and reactive components using the following procedure. We first obtained the magnitude of the internal impedance using the relation $|z_{\rm int}| = \frac{V_{\rm oc}}{I_{\rm sc}}$, with $V_{\rm oc}$ and $I_{\rm sc}$ measured at 40 rotations per second. We then measured the real part $r_{\rm int}$ directly by connecting a multimeter to the generator terminals in resistance measurement mode. The remaining imaginary part of the internal impedance was calculated using $x_{\rm int} = \sqrt{|z_{\rm int}|^2 - r_{\rm int}^2}$. The measured values of $V_{\rm oc}$, $I_{\rm sc}$, and $r_{\rm int}$, as well as the calculated $x_{\rm int}$, are as follows:

- **Generator 1**: $V_{\rm oc} = 1.85\,{\rm V}$, $I_{\rm sc} = 0.50\,{\rm A}$, $r_{\rm int} = 1.6\,\Omega$, $x_{\rm int} = 3.34\,\Omega$.
- **Generator 2**: $V_{\rm oc} = 1.90\,{\rm V}$, $I_{\rm sc} = 0.51\,{\rm A}$, $r_{\rm int} = 1.6\,\Omega$, $x_{\rm int} = 3.36\,\Omega$.
- **Generator 3**: $V_{\rm oc} = 1.79\,{\rm V}$, $I_{\rm sc} = 0.50\,{\rm A}$, $r_{\rm int} = 1.6\,\Omega$, $x_{\rm int} = 3.20\,\Omega$.

The mean and the standard deviation among the three generators are $V_{\rm oc} = 1.85 \pm 0.055\,{\rm V}$, $I_{\rm sc} = 0.50 \pm 0.058\,{\rm A}$, $r_{\rm int} = 1.6 \pm 0.0\,\Omega$, and $x_{\rm int} = 3.30 \pm 0.087\,\Omega$. Note that the measured internal impedances of our generators would be called the synchronous impedance in the power systems literature, since $I_{\rm sc}$ is measured at a steady speed. This quantity is usually used to model the steady-state synchronous dynamics after a short period of transients following a short circuit, while the so-called transient impedance is used to model the transients. For our generators, however, we found no detectable transient, implying that the transient impedance is essentially equal to the synchronous impedance. Therefore, we used the $z_{\rm int}$ measured by the above procedure in our analysis of short-term dynamics.

Supplementary Figures

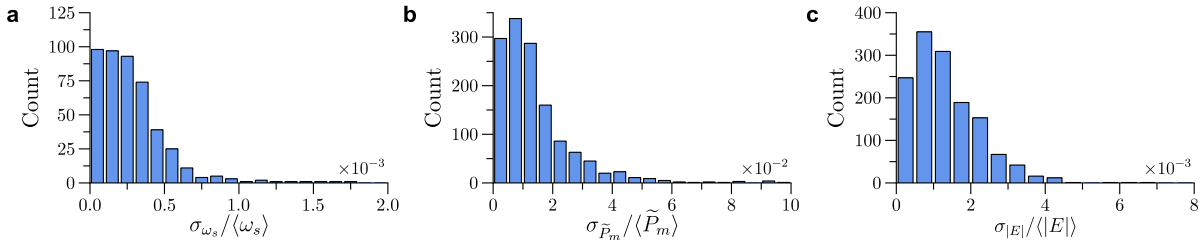

Supplementary Fig. 1: **Validation of model assumptions. a–c**, Histograms of normalized fluctuations for the parameters ω_{s} (**a**), $\widetilde{P}^{(\mathrm{pu})}_{\mathrm{m},i}$ (**b**), and E_i (**c**) (defined in Sec. S1). We quantify experimental fluctuations of a given parameter q of a given generator in a given time-series segment by $\sigma_q/\langle q\rangle$, where σ_q and $\langle q\rangle$ are the standard deviation and average, respectively, of the measured instantaneous values of q across the segment. The histograms, taken over all generators and over all time-series segments for each parameter, indicate that the (relative) magnitude of fluctuations in these parameters is approximately constant in each time-series segment, validating the corresponding assumptions underlying Eq. (1) of the main text.

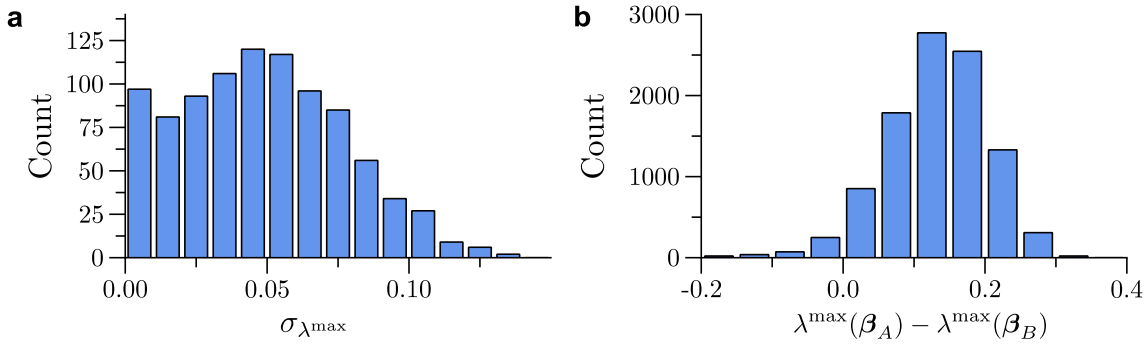

Supplementary Fig. 2: **Robustness of measured stability improvement. a**, Distribution of $\sigma_{\lambda^{\max}}$, the standard deviation of $\lambda^{\max}$ as it varies along the trajectory in a given segment, where $\lambda^{\max}$ is computed using the instantaneous δ_i^* values at each data point in the segment. **b**, Histogram of predicted stability improvement $\lambda^{\max}(\boldsymbol{\beta}_A) - \lambda^{\max}(\boldsymbol{\beta}_B)$ when the dynamical parameters of the generators are randomly perturbed (using 10,000 realizations). The specific parameters perturbed were V_{oc}, I_{sc}, and J for each generator (defined in Secs. S1, S2.2, and S2.3). The perturbations were drawn from the normal distribution having the mean and the standard deviation of the measured values of a given parameter of each generator (see Sec. S2.3 and Supplementary Fig. 5). The vast majority of the realizations lead to a measurable stability difference between the two $\boldsymbol{\beta}$ configurations, showing that converse symmetry breaking is observable and robust even under realistic uncertainties in the state and parameters of the system.

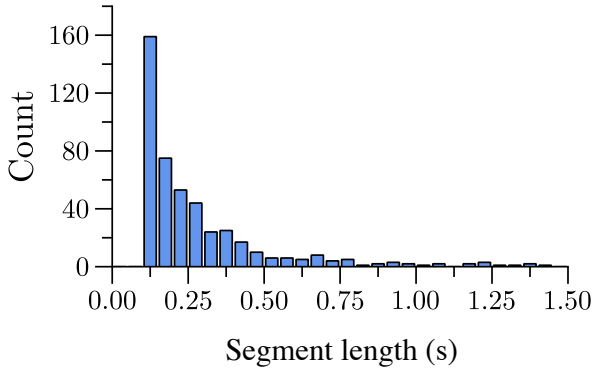

Supplementary Fig. 3: **Length distribution of time-series segments.** The histogram shows the distribution of the lengths of the time-series segments used in the analysis shown in Fig. 3 (for both the $\boldsymbol{\beta}_A$ and $\boldsymbol{\beta}_B$ configurations).